Available online at www.sciencedirect.com
SCIENCE DIRECT®
International Journal of Plasticity 22 (2006) 581–601
INTERNATIONAL JOURNAL OF Plasticity
www.elsevier.com/locate/ijplas

Thermo-mechanical large deformation response and constitutive modeling of viscoelastic polymers over a wide range of strain rates and temperatures

Akhtar S. Khan *, Oscar Lopez-Pamies [1], Rehan Kazmi

Department of Mechanical Engineering, University of Maryland Baltimore County, Baltimore, MD 21250, USA

Received 14 April 2005
Available online 28 November 2005

Abstract

A phenomenological one-dimensional constitutive model, characterizing the complex and highly nonlinear finite thermo-mechanical behavior of viscoelastic polymers, is developed in this investigation. This simple differential form model is based on a combination of linear and nonlinear springs with dashpots, incorporating typical polymeric behavior such as shear thinning, thermal softening at higher temperatures and nonlinear dependence on deformation and loading rate. Another model, of integral form, namely the modified superposition principle (MSP), is also modified further and used to show the advantage of the newly developed model over MSP. The material parameters for both models are determined for Adiprene-L100, a polyurethane based rubber. The constants once determined are then utilized to predict the behavior under strain rate jump compression, multiple step stress relaxation loading experiment and free end torsion experiments. The new constitutive model shows very good agreement with the experimental data for Adiprene-L100 for the various finite loading paths considered here and provides a flexible framework for a three-dimensional generalization.

Keywords: Polymers; High strain rate; Modeling; Temperature dependence; Viscoelasticity; Finite deformation

* Corresponding author. Tel.: +1 410 455 3301; fax: +1 410 455 1052.
E-mail address: khan@umbc.edu (A.S. Khan).
[1] Department of Mechanical Engineering and Applied Mechanics, University of Pennsylvania, Philadelphia, PA 19104-6315, USA.

0749-6419/$ - see front matter © 2005 Published by Elsevier Ltd.
doi:10.1016/j.ijplas.2005.08.001

1. Introduction

Polymers are proven to have an enormous and intriguing range of desirable features. This is basically due to the linking and arrangement of their smaller units or monomers. The synthesis, arrangement and conformations of these monomeric units result in a class of materials with a range of varied properties (Painter and Coleman, 1997). The many attractive mechanical characteristics of polymers have made it desirable to choose these materials over traditional materials for numerous types of applications such as binder-constituent in explosives, load-bearing components, jet engines modules, etc. As the uses of polymers increase, a thorough understanding of the mechanical behavior of these materials becomes vital in order to perform innovative and economical designs of various components.

Considerable progress has been made in developing mathematical models for the small strain regime under a specific narrow spectrum of strain rates and temperatures (see the monographs by Lockett, 1972; Christensen, 1982). Much less progress has been made for multiaxial finite deformation behavior under a wide range of strain rates and temperatures from a continuum point of view. Continuum approach ignores the molecular nature of matter and treats it in terms of laws of elasticity for solids and laws of fluid dynamics and viscous flow for liquids (Ogden, 1997). Polymers, however, have more complicated properties as they display both elastic and viscous type response at different strain rates and temperatures. Some literature though can be found for modeling large deformations in polymers like Haupt et al. (2000); Ehlers and Markert (2003). Haupt et al. (2000) have proposed a model for finite viscoelasticity. The model is based on a multiplicative split of the deformation gradient into a thermal and mechanical part. However, they did not apply to experimental observations, and thus validity of their model is not proven. Reese (2003) has also developed a material model for the thermo-viscoelastic behavior of rubber-like polymers. It is based on transient network theory. In the case of micromechanics based modeling, a high degree of refinement has been reached to model finite deformation of polymers. However, these micromechanics based models are extremely difficult to use and rely on assumptions that have been questioned (e.g., Argon et al., 1995). Some of these micromechanical models can be found in the literature (Boyce et al., 1988; Bergstrom and Boyce, 1998; Reese, 2003; Drozdov and Dorfmann, 2003; Makradi et al., 2005). There are also other studies that deal with polymer modeling based on over stress (Krempl and Khan, 2003; Colak, 2005). Some readers may find a paper by Liu et al. (2006) interesting, which is based on modeling of shape-memory polymers.

The main objective of this paper is to develop a simple and flexible phenomenological constitutive model to characterize the observed time and temperature dependent mechanical response of soft polymers under finite deformation. The developed model is shown to predict the observed behavior of Adiprene-L100, a polyether urethane-based rubber, under various one-dimensional, time as well as temperature dependent loading experiments. Extensive uniaxial experimental data with the experimental details for this polymer can be found in Lopez-Pamies and Khan (2002). In that study, the dimensions of the uniaxial specimens were 1.00 in. (25.4 mm) in length and 0.80 in. (20.5 mm) in diameter. Hollow tubular specimens were used to perform the free end torsion experiments. The inner diameter of the specimens was approximately 0.55 in. (13.97 mm) and the outer diameter was 0.675 in. (17.145 mm). The length of the specimen was approximately 0.85 in. (21.59 mm). All the quasi-static experiments were performed under displacement/angle

control mode on a MTS axial/torsional servo-hydraulic 810 system. Dynamic experiment was performed using the conventional compression split-Hopkinson pressure bar apparatus. The specimen for the dynamic experiment was solid disk of Adiprene-L100 of 0.42 in. (10.67 mm) diameter and 0.13 in. (3.30 mm) thickness. The detailed description of the dynamic setup and SHPB technique can be found in previous papers (Liang and Khan, 1999; Khan and Zhang, 2001).

Previous studies (Lopez-Pamies and Khan, 2002; Gray et al., 1997) have confirmed that the material response of Adiprene- L100 is almost totally viscoelastic, with very little viscoplastic deformation. As a result, only viscoelastic modeling is considered in this paper.

2. Classical linear theory of viscoelasticity

Substantial development has been attained in modeling the small strain regime behavior of polymeric materials. The well-known classical linear theory of viscoelasticity (Flügge, 1967; Christensen, 1982) describes fairly well the characteristic behavior of polymers such as creep, relaxation, and loading-rate dependence in a qualitative manner. However, the quantitative description by using this linear viscoelasticity is generally limited to very narrow loading-rate and temperature regimes.

The classical linear theory of viscoelasticity can basically be presented by two major forms: hereditary integrals or differential forms. Even though the differential constitutive forms are not as general (Lockett, 1972) as the hereditary integral representations, they are more commonly used. This fact is mostly due to the more appealing usage of parameters such as stress/strain and stress/strain rates, as opposed to relaxation and creep kernels. Furthermore, the differential forms can be directly related to the intuitive spring and dashpot diagrams. It is recalled here that a linear spring constitutive equation is of the form $\sigma_s = E\varepsilon_s$, where σ_s and ε_s are the stress and the strain in the spring, respectively. E is the constant modulus of the spring and implies a linear elastic stress–strain relationship. Similarly, a linear dashpot constitutive equation is of the form $\sigma_d = \eta\dot{\varepsilon}_d$, where σ_d and $\dot{\varepsilon}_d$ are the stress and strain rate in the dashpot, respectively. η is the constant viscosity and implies a Newtonian viscous effect.

Since the origin of the infinitesimal viscoelastic theory, numerous modifications have been introduced to improve on predictions of real material behavior from different combinations of springs and dashpots (Lubarda et al., 2003; Bardenhagen et al., 1997). We consider now a popular combination of springs and dashpot, the so-called standard solid model, shown by Fig. 1 and composed of a Maxwell element (linear spring and dashpot in series) with a linear spring in parallel. The stress in the standard solid is the sum of the

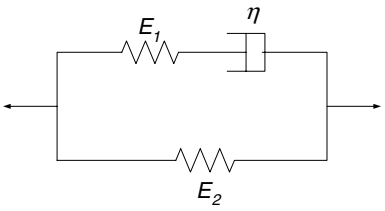

Fig. 1. Three-element standard solid model.

stresses in the Maxwell element and the linear spring. The governing equation for the system can be readily derived as

$$\frac{\eta}{E_1}\frac{\mathrm{d}\sigma}{\mathrm{d}t}+\sigma=\frac{\eta}{E_1}(E_1+E_2)\frac{\mathrm{d}\varepsilon}{\mathrm{d}t}+E_2\varepsilon. \tag{1}$$

Here η, E_1, and E_2 are material constants; σ and ε are the stress and strain, respectively. Note the structure of the constitutive equation (1). Only the current strain and stress, and current strain and stress rates are the arguments of the system. It can be shown that the standard solid model captures qualitatively the trends of general material behavior such as creep, stress-relaxation, and loading-rate sensitivity, even for large strains. This point will be elaborated further and utilized later to develop a new constitutive model. Eq. (1) is just a particular equation for the specific case of the standard solid model. More generally, any linear viscoelastic differential model can be expressed as follows (Christensen, 1982):

$$\left(p_0+p_1\frac{\partial}{\partial t}+p_2\frac{\partial^2}{\partial t^2}+\cdots\right)\sigma(t)=\left(q_0+q_1\frac{\partial}{\partial t}+q_2\frac{\partial^2}{\partial t^2}+\cdots\right)\varepsilon(t), \tag{2}$$

where p_i and q_i are material constants. The differential form of Eq. (2) solely involves current strain, stress, strain rates, stress rates and higher derivatives. These arguments, as already discussed, have a clear physical insight. In addition, the material parameters in Eq. (2) can be readily determined from simple experiments.

Some important observations should be made regarding Eq. (2). Firstly, the time dependent component of stress relaxation processes is described by a summation of exponential terms, namely

$$\sigma(t)=c_0+c_1\mathrm{e}^{-\frac{t}{\tau_1}}+c_2\mathrm{e}^{-\frac{t}{\tau_2}}+\cdots+c_n\mathrm{e}^{-\frac{t}{\tau_n}}, \tag{3}$$

where c_i are constants and τ_i are relaxation times ($i=1,\ldots,n$). It has been noted that the time dependent component of the stress relaxation of polymers, say $g(t)$, very often follows a simple power law-type behavior $g(t)=t^n$ (Lockett, 1972). In order for Eq. (3) to adequately approximate this feature, many exponential terms may be required. In essence, linear viscoelastic differential constitutive relations necessitate a large number of material parameters to approximate actual transient stress relaxation responses. Also, the power law behavior of creep and relaxation can be represented using the concept of fractional derivatives as shown by Lion (2001) and Lion and Kardelky (2004). Furthermore, polymers do not exhibit constant viscosity as assumed by the linear dashpot constitutive relation $\sigma_\mathrm{d}=\eta\dot{\varepsilon}_\mathrm{d}$. Instead, they exhibit shear thinning (or more rarely, shear thickening). As the name suggests, shear thinning implies that the viscosity decreases with increasing strain rate. This phenomenon has been attributed to the variation of the rate of polymer chain "disentanglement" with increasing strain rate (Painter and Coleman, 1997). Also, under different temperature conditions they are also known to exhibit totally different responses. At low temperatures they behave in a brittle elastic manner; at high temperatures, much above the glass transition the behavior is more 'rubbery' (viscoelastic). There is a huge drop in modulus when the temperature is increased above the glass transition temperature, indicating a shift in behavior from 'glassy' to 'rubbery' (Bardenhagen et al., 1997). Because of these peculiar mechanical properties of polymeric materials, the linear theory of viscoelasticity is unable to model closely the observed response and thus there is a need for a non-linear theory of viscoelasticity.

3. Nonlinear viscoelasticity

Many nonlinear theories of viscoelasticity have been proposed (Lockett, 1972; Christensen, 1982). Most of them follow a similar pattern. Analogous to the linear case, they are based on the axiom that the stress in a viscoelastic material depends on the entire deformation history; or alternatively, the strain in a viscoelastic material depends on the entire stress history. The stress–strain constitutive models can be put in the three major groups: the multiple integral, the single integral, and the differential relations. Some of these relations have a physical foundation whereas others are purely empirical.

The most general multiple integral constitutive relation for a nonlinear viscoelastic material is given by the Green–Rivlin theory (Green and Rivlin, 1957). This constitutive relation was developed around the dependence of the current stress (strain) state on the entire history of the deformation (stress), with the assumption of material isotropy. Under these hypothesis and further mathematical constraints, Green and Rivlin developed a constitutive law based on an expansion of multiple integrals with multivariable relaxation functions as kernels. A convenient form is (Lockett, 1972):

$$\begin{aligned}\underline{\Sigma}(t) = &\int_{-\infty}^{t} [\underline{I}\cdot\phi_1\cdot T_1 + \phi_2\cdot\underline{M_1}]\,\mathrm{d}\tau_1 + \int_{-\infty}\int [\underline{I}\cdot\phi_3\cdot T_1\cdot T_2 + \underline{I}\cdot\phi_4\cdot T_{12}\\ &+ \phi_5\cdot T_1\cdot\underline{M_2}\phi_6\cdot\underline{M_1}\cdot\underline{M_2}]\,\mathrm{d}\tau_2 + \int_{-\infty}\int\int [\underline{I}\cdot\phi_7\cdot T_{123} + \underline{I}\cdot\phi_8\cdot T_1\cdot T_{23}\\ &+ \phi_9\cdot T_1\cdot T_2\cdot\underline{M_3} + \phi_{10}\cdot T_{12}\cdot\underline{M_3} + \phi_{11}\cdot T_1\cdot\underline{M_2}\cdot\underline{M_3}\\ &+ \phi_{12}\cdot\underline{M_1}\cdot\underline{M_2}\cdot\underline{M_3}]\,\mathrm{d}\tau_3 + \cdots,\end{aligned} \tag{4}$$

where

$$\begin{aligned}&\mathrm{d}\tau_x = \mathrm{d}\tau_1\,\mathrm{d}\tau_2\,\mathrm{d}\tau_3\ldots\mathrm{d}\tau_x,\\ &\underline{M_x} = \dot{\underline{E}}(\tau_x),\quad T_x = \mathrm{tr}\,(\underline{M_x}),\\ &T_{xy} = \mathrm{tr}\,(\underline{M_x}\underline{M_y}),\quad T_{xyz} = \mathrm{tr}\,(\underline{M_x}\underline{M_y}\underline{M_z}).\end{aligned} \tag{5}$$

For hereditary materials the material functions, or stress relaxation functions, ϕ_1 and ϕ_2 are functions of $t-\tau_1$; $\phi_3,\ldots,\phi_6$ are functions of $t-\tau_1, t-\tau_2$; $\phi_7,\ldots,\phi_{12}$ are functions of $t-\tau_1, t-\tau_2$, and $t-\tau_3$. The polynomial expression in Eq. (4) may be continued to higher orders where the applicability becomes totally unpractical. Eq. (4) is one form of the Green–Rivlin Theory. The explicit expression in Eq. (4) involves many material functions and it has been shown that the determination of such functions is nearly impossible as it requires unrealistic numbers of experiments (of the order of hundreds). In synthesis, the multiple integral constitutive relations introduced by the Green–Rivlin Theory are based on very reasonable constraints. The behavior is assumed isotropic as well as the mathematical assumptions involved with the development of the theory are not restrictive. These reasonable constraints introduce a high complexity in the model. The material functions involve in Eq. (4) depend on several integration variables. Also, the experimental determination of these multivariable material functions requires an impractical number of tests. The complexity of this model and the large amount of experimental data required

for the determination of the material parameters resulted in a very limited use. Despite this fact, the Green–Rivlin theory provides an idealistic nonlinear viscoelastic theory from which other models can be derived and compared.

Significant efforts have been made to reach more applicable models for nonlinear viscoelastic materials than the Green–Rivlin theory (McGuirt and Lianis, 1970; Findley, 1968; Pipkin and Rogers, 1968). Smart and Williams (1972) have compared three single integral models which are much easier to implement. A number of physical and semi-empirical single integral constitutive relations have also been proposed (Caruthers et al., 2004). These models are also mathematically very complicated to use. Here, one of these single integral models, the modified superposition principle (MSP), is presented and utilized to model Adiprene-L100. The reason to consider this single integral form of constitutive model in particular is based on its simplicity and foundation. More specifically, the idea is to compare an existing semi-empirical stress–strain constitutive law to the phenomenological differential constitutive model developed in this study.

3.1. The modified superposition principle

The MSP was first introduced by Leaderman in the early 1940's (Smart and Williams, 1972). After some experimental work on polymeric fibers, Leaderman concluded that the strain behavior of the fibers under creep could be separated into time and stress dependent parts (Ward and Sweeney, 2004), that is

$$\varepsilon(t) = k\sigma + h(\sigma)D(t) \tag{6}$$

with an associated convolution integral

$$\varepsilon(t) = k\sigma(t) + \int_0^t D(t-\tau)\,\frac{\mathrm{d}h(\sigma(\tau))}{\mathrm{d}\tau}\,\mathrm{d}\tau, \tag{7}$$

where $\varepsilon(t)$ and $\sigma(t)$ are the engineering strain and true stress, respectively; k is a material constant, $h(\sigma)$ and $D(t)$ represent the separation of the stress and time dependent parts of the creep response. This was named the modified superposition principle by Lai and Findley (1968). Note that the true stress $\sigma(t)$, i.e., stress with respect to the deformed configuration is being used in Eq. (7). Leaderman also considered formulations in terms of engineering stress, i.e., the stress with respect to the undeformed configuration, as well as some other nonlinear stress measures (see Lockett, 1972 for further details). The modified superposition principle can also be represented with the stress as a functional of strain history. Since it is a nonlinear theory, there are no analytical inversion formulae as in linear viscoelasticity. The stress response of a nonlinear viscoelastic material under relaxation, in a manner similar to Eq. (6), could be separated into a time dependent, $D(t)$, and a strain dependent, $h(\varepsilon)$, part, such that

$$\sigma(t) = k\varepsilon + h(\varepsilon)D(t) \tag{8}$$

with the corresponding convolution integral

$$\sigma(t) = k\varepsilon(t) + \int_0^t D(t-\tau)\,\frac{\mathrm{d}h(\varepsilon(\tau))}{\mathrm{d}\tau}\,\mathrm{d}\tau. \tag{9}$$

Eq. (9) represents the MSP-type constitutive relation utilized later to model the response of Adiprene-L100.

3.2. Approach to the development of the modified standard solid model (MSSM)

A popular approach to model nonlinear finite viscoelastic behavior has been the use of differential constitutive relations (Lubarda et al., 2003; Bardenhagen et al., 1997). Various differential forms are based on spring and dashpots combinations, i.e., the foundations of these models are on linear viscoelastic constitutive relations. The standard solid model, Fig. 1, is one such type of model. The constitutive equation for this model has already been shown by Eq. (1)

Bardenhagen et al. (1997) have also considered Eq. (1) as a starting point to model finite deformation of polymers. However, their work was primarily focused on the generalization to three-dimensional case of both viscoelastic and viscoplastic deformation regimes.

In order to acquire more insight into the behavior of the standard solid model, it is important to consider numerical simulations for constant strain rate loading and stress relaxation processes, as well as the corresponding analytical solutions to these loadings. The analytical solution for constant strain rate loading (i.e., $\dot{\varepsilon} = \dot{\varepsilon}_0$) is readily determined from Eq. (1) yielding

$$\sigma = E_2\varepsilon + \eta\dot{\varepsilon}_0 - \eta\dot{\varepsilon}_0 \mathrm{e}^{-E_1\varepsilon/\eta\dot{\varepsilon}_0}. \tag{10}$$

Note that the initial modulus for any given constant strain rate loading is simply the sum of the moduli of the two linear springs in the model. The asymptotic behavior for sufficiently large strains is linear, $\sigma(\infty) = E_2\varepsilon + \eta\dot{\varepsilon}$. Fig. 2(a) depicts the strain rate sensitivity of the standard solid model (see also Bardenhagen et al., 1997). From this figure as well as from Eq. (10) it is clearly concluded that the standard solid model under constant strain rate and finite deformation presents a bilinear behavior, that is, linear effective modulus and linear asymptotic strain rate hardening. This is a good initial approximation to the observed behavior of typical polymeric materials under such a loading. Similarly, the analytical solution for single-step stress relaxation processes (i.e., $\varepsilon = \varepsilon_0 H(t)$; where $H(t)$ is the Heaviside function) readily follows from Eq. (1)

$$\sigma(t) = E_2\varepsilon_0 + E_1\varepsilon_0 \mathrm{e}^{-E_1 t/\eta}. \tag{11}$$

Fig. 2(b) shows the schematic of stress-relaxation exhibited by using the standard solid model. Again, the trends of typical polymeric behavior are well captured by this simple model making it a good starting point for the development of an advanced model. However, in order to adapt and exploit the differential form of the standard solid model to characterize finite nonlinear deformation of real polymers, various changes with regards to the definitions of stress, stress rate, strain and strain rate need to be introduced for finite deformation. The engineering strain ε needs to be replaced by adequate and objective measure for the finite deformation regime. The selected parameter chosen for strain should be based on the deformed configuration. There exist several choices for deformation measures, i.e., true strain $\underline{\varepsilon}_{\mathrm{true}} = \ln(\underline{V})$, where $\underline{V}$ is the left Cauchy tensor, the Lagrangean Almansi–Hemel strain ($\underline{\mathrm{E}}$), the Eulerian Almansi–Hemel ($\underline{\mathrm{e}}$) strain, etc. For this study, true strain was selected as the most appropriate unit for the strain measure. Also, the true or Cauchy stress is being utilized as the measure of the response of the material under finite deformation.

In the determination of the constitutive equation for the modified standard solid model (MSSM), various springs and dashpots were utilized. Fig. 3 depicts the arrangement used for this study. It basically represents a Maxwell element connected in parallel with a

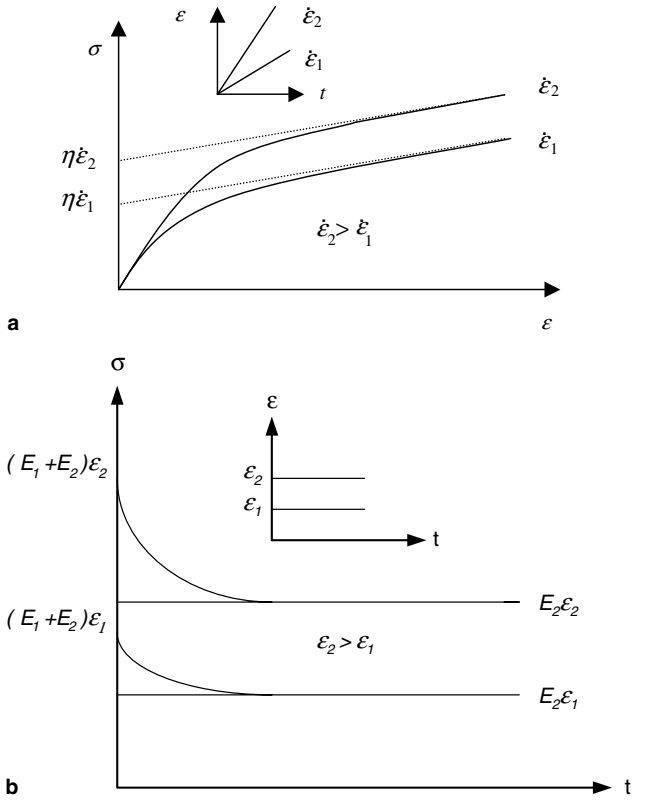

Fig. 2. (a) Strain rate sensitivity of the standard solid model. (b) Relaxation response of the standard solid model.

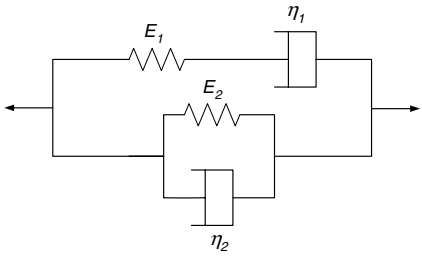

Fig. 3. Rheological schematic of the modified standard solid model.

Kelvin solid (except E_2 is not a linear spring). The spring E_1 is considered to be a material constant dependent only on operating temperature, whereas the other spring, E_2, is assumed to be a nonlinear spring dependent on the level of deformation as well as temperature as a significant change in the modulus with temperature has been observed. The equation for viscosity used for the two dashpots in the study was not taken to be a constant quantity, rather it was considered to be a function of strain rate and temperature. This is consistent with the term used by other researchers on polymers, as viscosity has

been known to depend on both, rate of loading as well as the temperature of the material. The original form of the viscosity term, which has been modified here, was taken from Bird et al. (1977). Similar equations have been used by Khan et al. (2004) and Bardenhagen et al. (1997) previously. The modification was performed to predict the actual viscosity in the material for a specific strain rate as well as the operating temperature of the polymer during the experiment. The modified viscosity function η, is given in the following form:

$$\eta(\dot{\varepsilon}, T) = \left[\eta_\infty + \frac{\eta_0 - \eta_\infty}{\left(1 + (a|\dot{\varepsilon}|)^2 - \left(\frac{|\dot{\varepsilon}|}{10^5}\right)^d\right)^b}\right]\left(\frac{T_r - T_{vf}}{T - T_{vf}}\right)^m, \tag{12}$$

where η_0 is the viscosity at zero strain-rate and η_∞ is the asymptotic viscosity at $\dot{\varepsilon} = \infty$. $\dot{\varepsilon}$ is the strain rate (s^{-1}) experienced by each dashpot (note that the strain rates in the two dashpots are not the same). The material parameters a, d and b serve to adjust the decay of shear thinning under increasing strain rate. The denominator is, however, never allowed to become negative. It is noted that the viscosity at zero strain-rate, potentially introduces physical insight into the constitutive model through the molecular weight of the polymer (Painter and Coleman, 1997). The material parameter, m, adjusts the response of viscosity of the polymer with different temperatures. Here, T_{vf} is the Vogel–Fulcher temperature term, taken from the well-known Vogel–Fulcher-Tammann Law, which relates viscosity as a function of temperature. T_{vf} is usually taken 50 K below the experimental glass transition temperature ($\sim T_g - 50$ K) for polymers (Rault, 2000). T_g is the glass transition temperature. T_r is the reference temperature or the room temperature in the present study. T is the temperature at which the experiment is performed. In case of Adiprene-L100 the glass transition temperature is 211 K (−80 °F). Overall, the temperature term used here is taken from the Khan–Huang–Liang equation (Khan et al., 2004), which has been successfully used to predict the viscoplastic response of metal and alloys.

The behavior of the two springs E_1 and E_2, for the standard solid model during stress relaxation, present a dependency on the strain, not on strain rate. Hence, it seems that the spring components of the modified standard solid model are composed of two distinct modes, the loading and the relaxation mode. Based on this idea, the springs E_1 and E_2 in the modified standard solid model are redefined in the following form:

$$E_1 = c_1\left(1 + \frac{T_r - T}{T_d}\right), \tag{13}$$

$$E_2 = c_2|\varepsilon|^{n_2}\left(1 + \frac{T_r - T}{T_d}\right) \tag{14}$$

Here, c_1, c_2, and n_2 are material parameters and $|\varepsilon|$ is the true stain of the material. T_r, T_d and T are the room, the melting or decomposition (~473 K) and the operating temperatures, respectively. Note that higher refinement on the dependence on the strain could be obtained by splitting E_1 in the same manner as E_2. It should also be emphasized that many other forms of nonlinearities, i.e., rubber elasticity, might be implemented instead of the simple power law utilized in Eq. (14). However, this would lead to a more complex model and correspondingly more number of material parameters.

Fig. 3 shows the "rheological" schematic of the modified standard solid model incorporating the new concepts discussed above. The constitutive equation of the developed constitutive model, for room temperature, may finally be expressed as

$$\frac{c_1}{\eta_1}\sigma + \dot{\sigma} = c_1\dot{\varepsilon} + \frac{c_1}{\eta_1}c_2\varepsilon^{(n_2+1)} + \frac{\eta_2}{\eta_1}c_1\dot{\varepsilon} + c_2(n_2+1)\varepsilon^{n_2}\dot{\varepsilon}. \tag{15}$$

In summary, the one-dimensional constitutive relation given by Eq. (15) characterizes the observed viscoelastic behavior of typical polymeric materials under finite deformation. The functional expressions, η_1 and η_2, are dependent on strain rate and temperature; they decrease with increasing strain rate (shear thinning) and temperature (see Eq. (12)). Nonlinearity characteristics of the stress relaxation process is incorporated via a nonlinear spring, this is represented by E_2. Moreover, the constitutive equation (15) represents a flexible framework for future generalizations to three-dimensional modeling.

The stress response of the polymer for constant loading (constant strain rate) experiments was determined by solving the governing differential equation. This solution of the differential equation for constant loading is given by the equation below:

$$\sigma = (\eta_1 + \eta_2)\dot{\varepsilon}\left(1 - \mathrm{e}^{-c_1\varepsilon/\eta_1\dot{\varepsilon}}\right) + c_2\varepsilon^{(n_2+1)}. \tag{16}$$

Also, based on the differential equation shown in (15), the stress drop during the room temperature relaxation is found out by substituting the strain rate equal to zero ($\dot{\varepsilon} = 0$). The stress in this case can be written as:

$$\sigma = c_2\varepsilon_0^{(n_2+1)} + \left(\sigma_0 - c_2\varepsilon_0^{(n_2+1)}\right)\mathrm{e}^{-c_1 t/\eta_1}. \tag{17}$$

In this case the viscosity term given by Eq. (12) reduces to $\eta(\dot{\varepsilon}, T) = \eta_0$ for experiments at reference temperature.

4. Results and discussion

4.1. Application of the modified form of MSP to Adiprene-L100

Fig. 4 shows the relaxation response of Adiprene-L100 at different levels of strain. The corresponding true stress versus time plot can be seen in Fig. 5. The bilinear behavior in the *Ln–Ln* space (see Fig. 6) exhibited by Adiprene-L100 during relaxation can be adequately captured in the stress–time space by the following expression

$$\sigma(t) = k_1\varepsilon^{r_1} + k_2 t^{r_2}\varepsilon, \tag{18}$$

where k_1, r_1, k_2, and r_2 are material parameters. Note that Eq. (18) does not perfectly fit the original MSP form given by Eq. (8); instead of having a first term linear in the strain, the actual behavior of the polymer has a power law. The incorporation of this new feature results into a more general, more flexible and more nonlinear constitutive relation. In essence, by assuming the stress–time relationship given by Eq. (18), the MSP constitutive equation reduces to

$$\sigma(t) = k_1\varepsilon^{r_1}(t) + \int_0^t k_2(t-\tau)^{r_2}\,\frac{\mathrm{d}\varepsilon(\tau)}{\mathrm{d}\tau}\,\mathrm{d}\tau. \tag{19}$$

The material parameters k_1, r_1, k_2, and r_2 for Adiprene-L100 were determined from the stress relaxation versus time data shown in Fig. 5. Table 1 shows the values of these

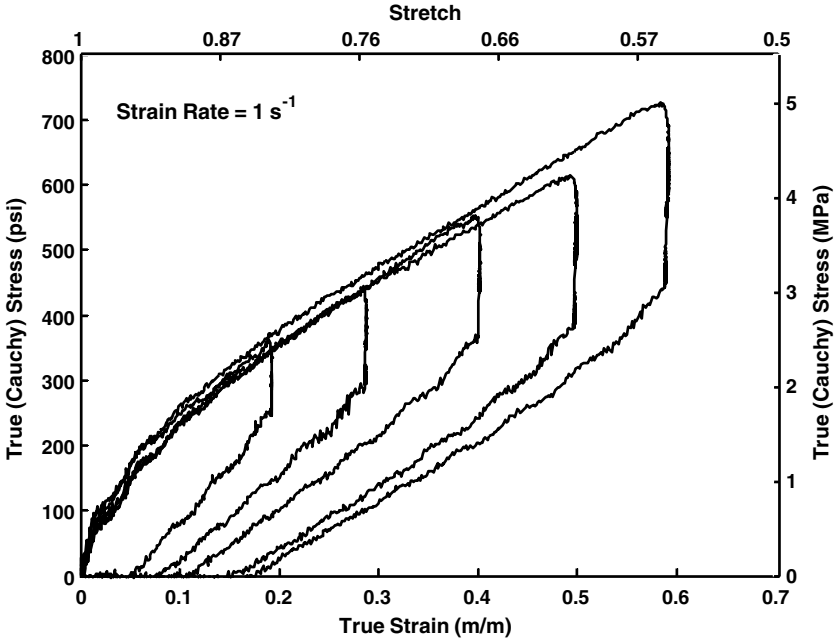

Fig. 4. True (Cauchy) stress–strain for relaxation experiments at different levels of strain at the engineering strain rate, or stretch rate, of 1 s^{-1} (compressive stresses and strains are assumed positive).

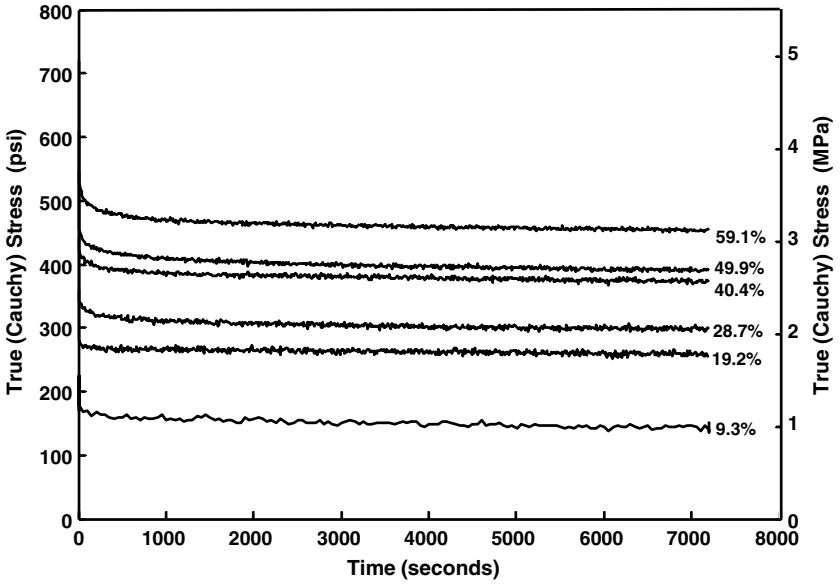

Fig. 5. True (Cauchy) stress–time for relaxation experiments at different levels of strain at the engineering strain rate, or stretch rate, of 1 s^{-1} (compressive stresses and strains are assumed positive).

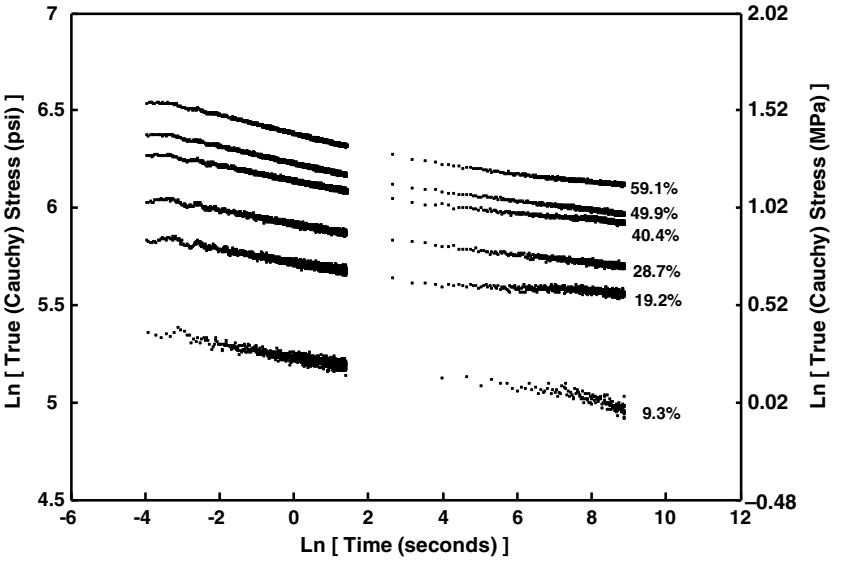

Fig. 6. *Ln–Ln* plot of the relaxation stress and time depicting a bilinear response (compressive stresses and strains are assumed positive).

Table 1
Material constants for Adiprene-L100 using MSP

k_1	272.31 psi
k_2	814.29 psi/s$^{-0.45}$
r_1	0.365
r_2	−0.045

parameters. Fig. 7 shows the experimental data along with the corresponding correlations from the modified form of MSP for all the stress relaxation experiments performed on Adiprene-L100. It is clear that the modified MSP constitutive model correlates very well with the stress relaxation response of Adiprene-L100 for small deformations; it is incapable to model the relaxation response at large deformations.

Fig. 8 shows the experimental true (Cauchy) stress versus true strain for constant strain rate loading on Adiprene-L100 at engineering strain rates (or stretch rates) of $\dot{\varepsilon}_e(\dot{\lambda}) = 10^{-5}$, 10^{-4}, 10^{-2}, 10^{0}, and 5000 s^{-1} along with the predictions from the MSP relation. It is clear from Fig. 8 that the MSP constitutive relation provides reasonable predictions for quasi-static strain rate deformations. However, it is unable to predict the actual behavior of the polymer Adiprene-L100 for deformations under dynamic strain rate regime.

During these experiments the engineering strain rate or stretch rate was held constant. Since, the true strain rate changes with deformation in the specimen, in model predictions as well as the viscosity functions it has been considered piecewise-constant for each 10% of deformation. The values of true strain rate at the two ends of each piecewise-constant intervals is averaged and used for that period.

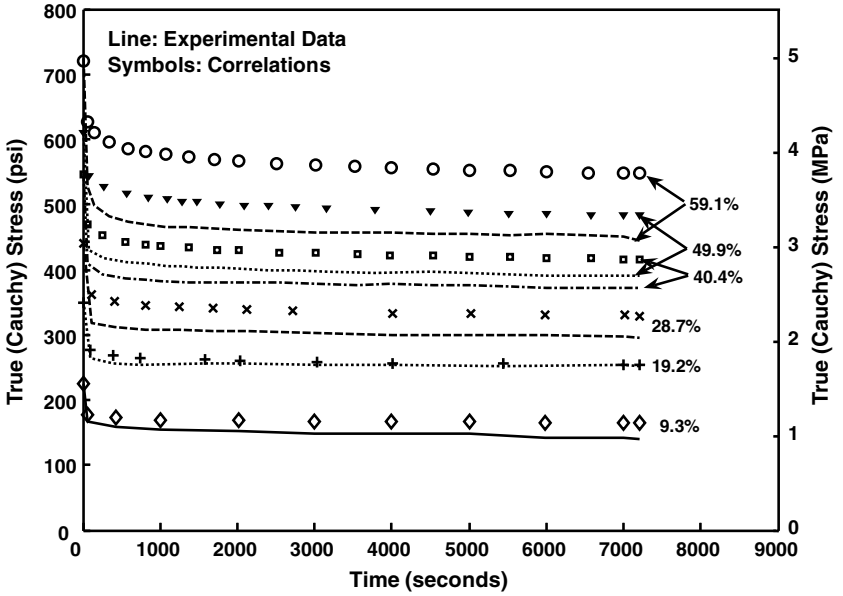

Fig. 7. MSP correlations during relaxation at different levels of strain (compressive stresses and strains are assumed positive).

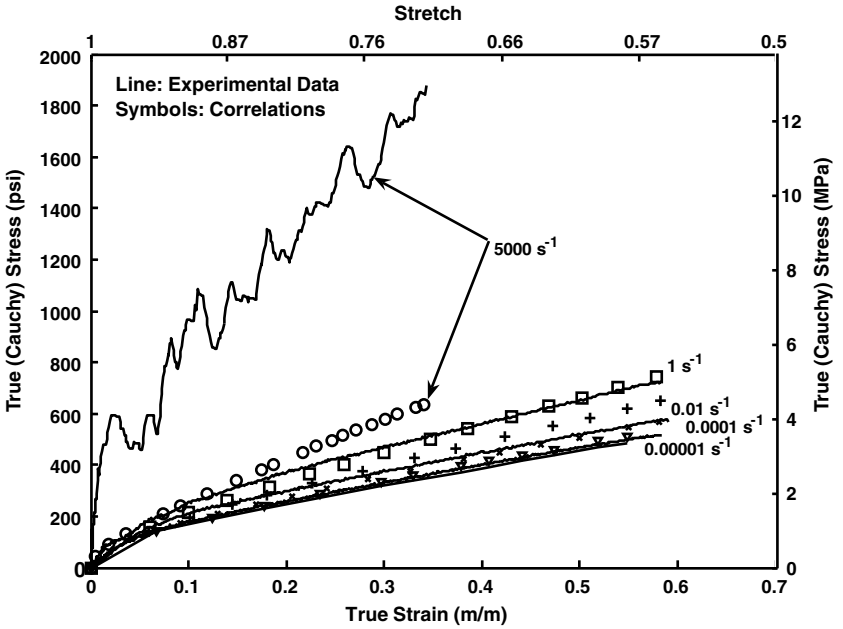

Fig. 8. MSP correlations during constant strain rate loading experiments (compressive stresses and strains are assumed positive). Strain-rates shown are corresponding engineering rates, or stretch rates.

An observation should be made before continuing with the approach and application of the differential model. In the preceding study of the modified form of MSP, the material constants were determined from stress relaxation data. During a stress relaxation experiment no changes in strain occur with time. On the other hand, during a constant strain or stress rate loading the strain does change with time and the rate of change of strain depends on the rate of loading. It could be argued that there are significant effects that are caused by changes of strain with time. Given that these effects do not arise during a stress relaxation response, models that use material parameters determined from this kind of experiments might overlook certain features of the material. When applicable, a possible improvement might be reached by using creep data, instead of stress relaxation data, to determine the material parameters of these models as shown by other researchers (Smart and Williams, 1972).

4.2. Application of the modified standard solid model to Adiprene-L100

The stress relaxation data (Fig. 5) were used to calculate different material parameters involved in Eq. (17) such as c_1, c_2, n_2 and η_0. σ_0 is the initial stress level at which the relaxation begins. Also, ε_0 represents the fixed strain at which the relaxation is performed. Least square optimization techniques were used to get these material parameters. Using Eqs. (13) and (14), with the temperature term as unity at room temperature the linear and non-linear spring constants were found out to be

$$E_1 = 1143 \text{ psi} \tag{20}$$

$$E_2(\varepsilon) = 630|\varepsilon|^{-0.385} \text{ psi}. \tag{21}$$

The viscosity function for the first dashpot at zero strain rate was found to be $\eta_1(0) = \eta_{(0)1} = 155{,}263$ psi s.

The model correlations obtained for the modified standard solid model along with the experimental data during relaxation are shown in Fig. 9. Note that the asymptotic behavior of the model presents a good correlation with the experimental data. The model captures even the transient part of the stress relaxation well. Although the results observed are quite close to observations still some scope for improvement is possible. In order to capture more accurately the relaxation response of Adiprene-L100 with the modified standard solid model, the addition of more relaxation times would be required. This could be accomplished by the addition of more Maxwell elements.

The remaining material parameters were determined from uniaxial compression experiments under quasi-static and dynamic loadings at constant strain rates. However, due to the nonlinearity introduced by Eq. (21), there is not a closed form solution for the constant strain rate deformation of the modified standard solid model. This, in turn, implies the impossibility of determining the material parameters η_∞, η_0, a, d and b analytically. Numerical methods need to be employed in order to obtain these material constants. The approach followed in this study was to apply a least square-fit type method to the experimental data on Adiprene-L100 under uniaxial compression at engineering strain rate (stretch rate) loadings of $\dot{\varepsilon}_e(\dot{\lambda}) = 10^{-5},\ 10^{-4},\ 10^{-2},\ 10^{0}$ and $5000\ \text{s}^{-1}$. The results yielded the following material constants for the two dashpots. Note that the equation is valid for room temperature experiments only and since the reference temperature for modeling is taken as room temperature, the temperature term in the viscosity equation becomes unity

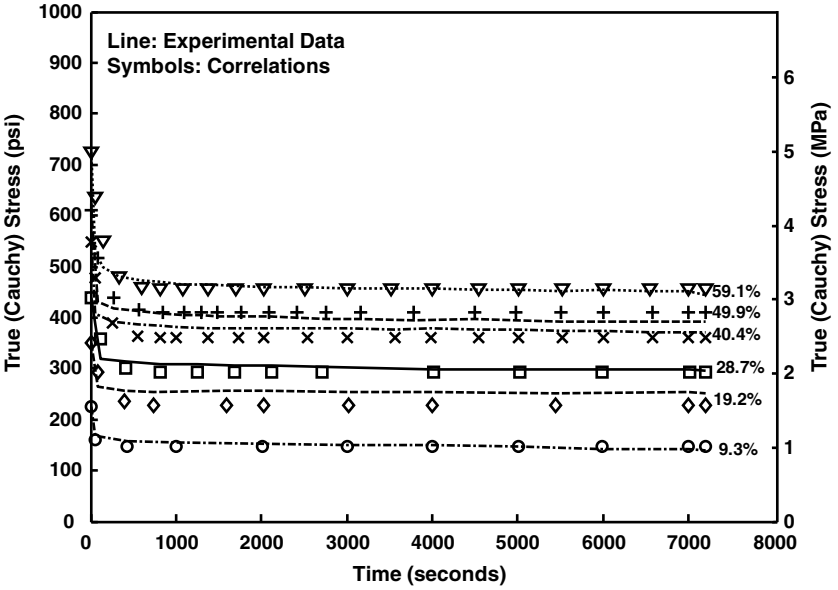

Fig. 9. True (Cauchy) stress–time for relaxation experiments with modified standard model correlations at different levels of strain at the engineering strain rate, or stretch rate, of 1 s^{-1} (compressive stresses and strains are assumed positive).

$$\eta_1 = \left[3.42 + \frac{155263 - 3.42}{\left(1 + (3790 \times |\dot{\varepsilon}_{d1}|)^2 - \left(\frac{|\dot{\varepsilon}_{d1}|}{10^5}\right)^2\right)^{0.414}} \right], \tag{22}$$

$$\eta_2 = \left[10.73 + \frac{151160 - 10.73}{\left(1 + (1411 \times |\dot{\varepsilon}|)^2 - \left(\frac{|\dot{\varepsilon}|}{10^5}\right)^2\right)^{0.907}} \right]. \tag{23}$$

The strain rate in dashpot 1 ($\dot{\varepsilon}_{d1}$) was determined iteratively by finding the stress in that particular arm (since the strain rate in that dashpot is the difference of the total strain rate ($\dot{\varepsilon}$) minus the strain rate experienced by the spring E_1). This strain rate was then utilized to find the new set of constants for the dashpot with the corrected strain rate. The strain rate in the spring, E_1, for the quasi-static experimental results was found to be almost negligible. However, for dynamic experiment it was found to be comparable to the strain rate in the dashpot. Fig. 10 shows the experimental true (Cauchy) stress versus true strain for the engineering strain rate (stretch rate) loading on Adiprene-L100 at strain rates of $\dot{\varepsilon}_e(\dot{\lambda}) = 10^{-5}$, 10^{-4}, 10^{-2}, 10^{0} and 5000 s^{-1} along with the correlations from the modified standard solid model. The behavior exhibited by the model is in reasonable agreement with the observed response for all quasi-static, as well as for the dynamic strain rate experiments. This implies that the dependency on the strain rate extracted from the quasi-static and dynamic strain rate loading experiments, i.e., the modified term, η, remains true in all the regimes.

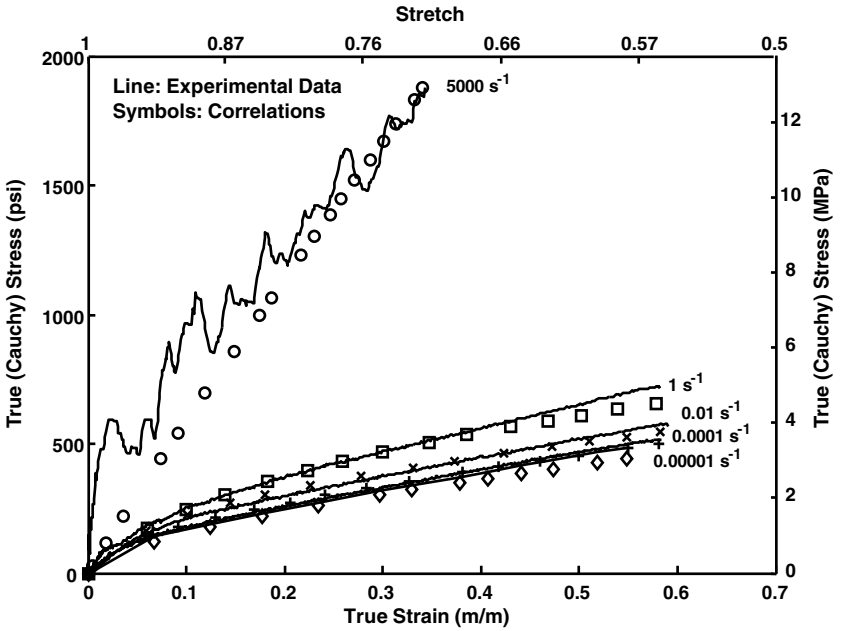

Fig. 10. True (Cauchy) stress–strain for uniaxial loadings with modified standard model correlations at different strain rates (compressive stresses and strains are assumed positive). Strain-rates shown are corresponding engineering rates, or stretch rates.

As mentioned before, the viscosity terms as well as the spring moduli were modified to include the effect of temperature on the response of the polymer (Eqs. (12)–(14)). This modification enabled modeling of the thermo-mechanical response of the polymer for large strains. While modeling the response of the polymer with different operating temperatures, the constants achieved during room temperature experiment correlations were kept constant at all times. The temperature sensitivity parameters, m, of the viscosity equations in both the dashpots were allowed to adjust themselves so as to produce good agreement with the experimental data. This was performed using a curve fitting scheme and least square optimization. The temperature response of the polymer along with the model correlations can be found in Fig. 11. The model was able to correlate well with the observed response even for the experiment performed above the glass transition temperature. The added temperature terms in the calculation of viscosity in the dashpots as well as the linear and nonlinear springs were able to capture the response reasonably well. All material constants for the newly developed viscoelastic model are shown in Table 2.

In order to further validate the capability of the modified standard solid model in producing good agreement of the observed response, predictions were performed on a compressive strain rate jump experiment on Adiprene-L100. In this experiment at room temperature, the engineering strain rate (stretch rate) loading of $\dot{\varepsilon}_e(\dot{\lambda}) = 10^{-4}\ s^{-1}$ was maintained constant up to a strain level of $\varepsilon = 24\%$, followed by a jump in the strain rate (stretch rate) to $\dot{\varepsilon}_e(\dot{\lambda}) = 10^{-2}\ s^{-1}$ and then maintained constant to a strain level of $\varepsilon = 45\%$. Constants determined utilizing the prior experiments were not changed to predict the response of the material under the given conditions. Fig. 12 illustrates the observed true (Cauchy) stress versus true strain response for the jump experiment along with the model

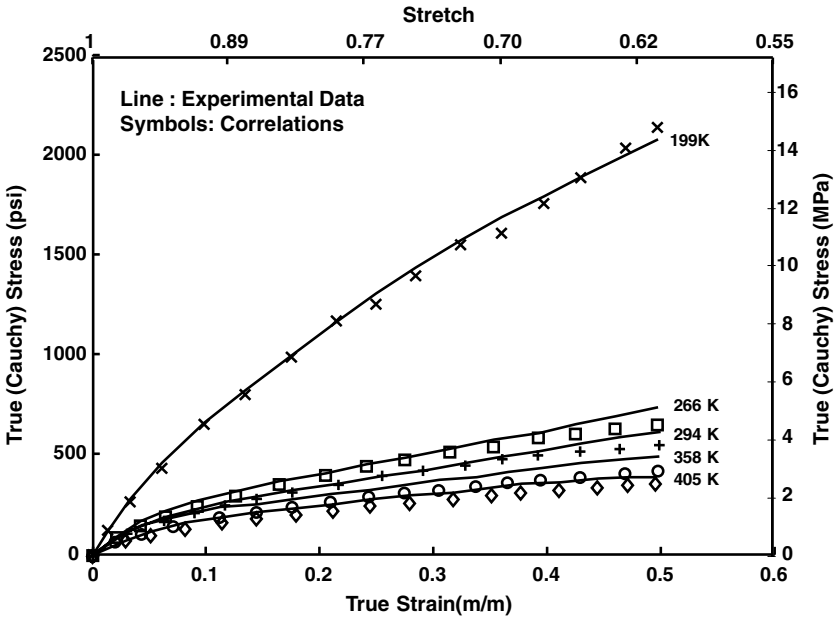

Fig. 11. Uniaxial experiments performed at $0.1\ s^{-1}$ engineering strain rate or stretch rate and at different temperatures along with the modified standard model correlations (compressive stresses and strains are assumed positive).

Table 2
Material constants for Adiprene-L100 using MSSM

c_1	c_2	n_2	$\eta_{(inf)1}$	$\eta_{(0)1}$	a_1	d_1	b_1	m_1
1143 psi	630 psi	−0.385	3.42 psi s	155,263 psi s	3790	2	0.414	1.84
$\eta_{(inf)2}$		$\eta_{(0)2}$	a_2	d_2		b_2		m_2
10.73 psi s		151,160 psi s	1411	2		0.907		5.48

predictions. The agreement between the two was found to be reasonably good. Further validation of the capability of the differential model was carried out for a multiple step stress relaxation experiment, which was performed at room temperature. Here again, the constants determined using the earlier set of experiments were not changed to predict the response of the material under constant rate of loading or during relaxation periods. Fig. 13 shows the experimental stress–strain relationship for a constant engineering strain rate(stretch rate) loading of $\dot{\varepsilon}_e(\dot{\lambda}) = 10^0\ s^{-1}$ with multiple step 2 h stress relaxation processes around $\varepsilon = 15\%$, 30%, 45% and 60% strain levels along with the corresponding predictions from the modified standard solid model. Again, the agreement between the experimental observations and the predictions from the model are very good.

Free end pure torsion experiments were performed on the Adiprene-L100 samples at different shear strain rates (see Fig. 14). The axial force was kept zero during the length of the experiment. The shear stress and strain values were calculated from the experimental data. The new modified viscoelastic model was used to calculate the effective von-Mises

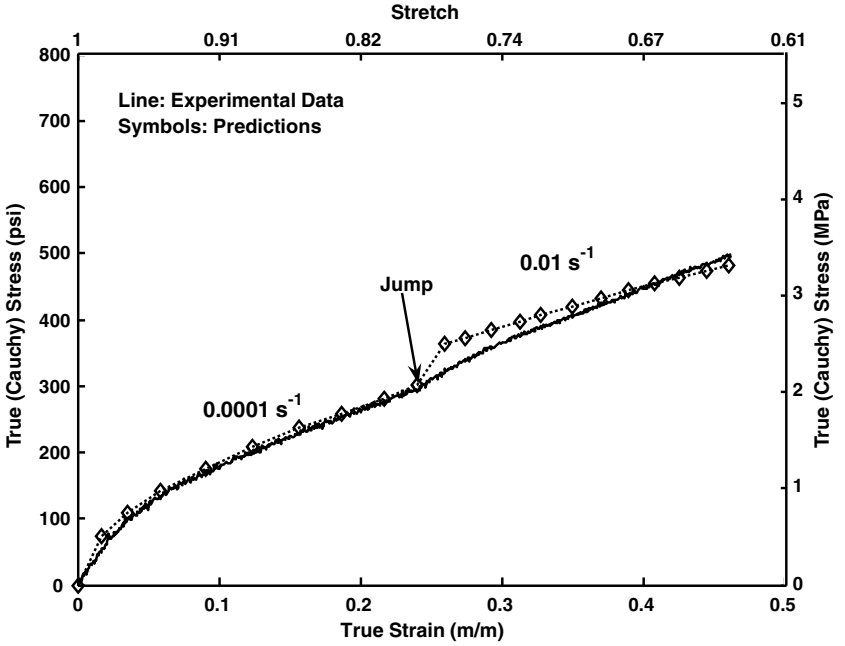

Fig. 12. True (Cauchy) stress–strain for strain rate jump (0.0001–0.01 s^{-1}) with modified standard solid model predictions (compressive stresses and strains are assumed positive). Strain-rates shown are corresponding engineering rates or stretch rates.

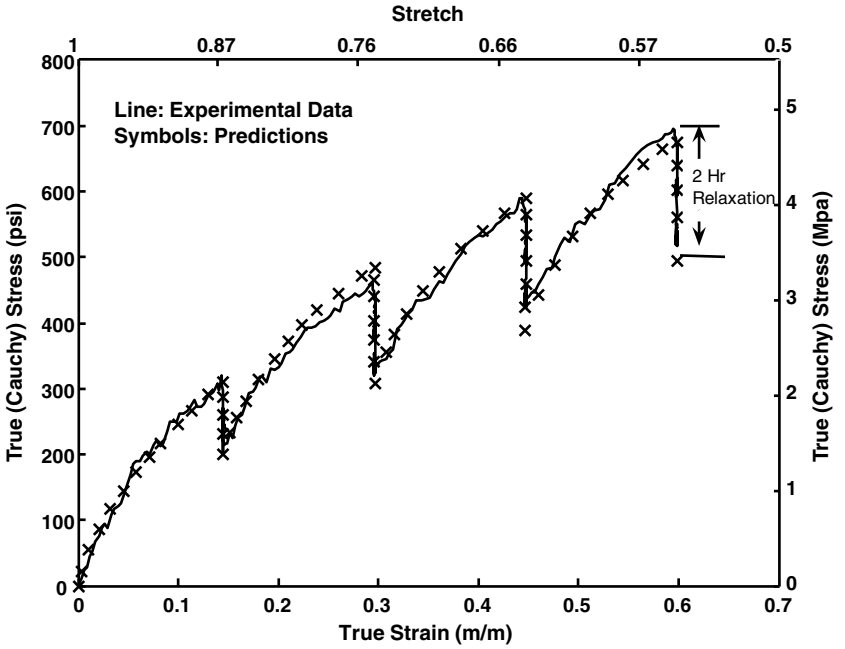

Fig. 13. Multiple step relaxation experiment at 1 s^{-1} engineering strain rate or stretch rate with 2 h relaxation period along with the modified standard model predictions (compressive stresses and strains are assumed positive).

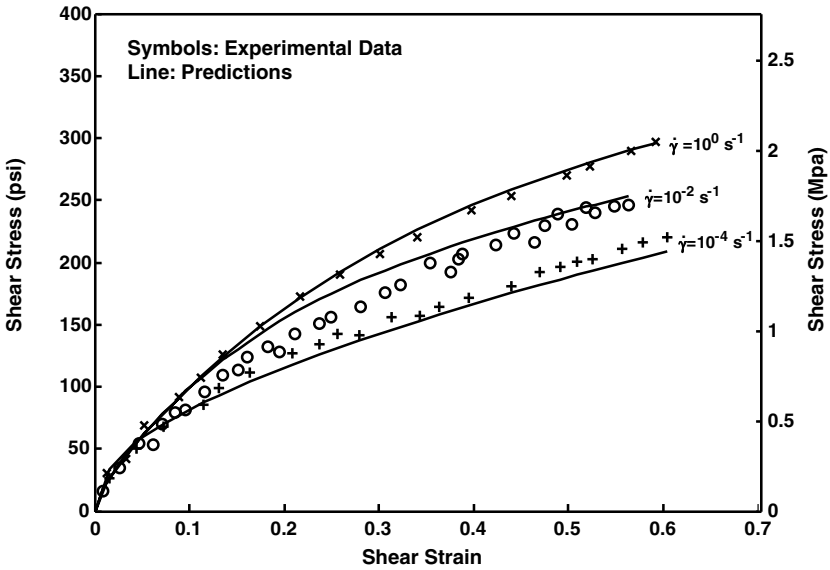

Fig. 14. Free end torsion experiments at various shear strain rates at room temperature along with model predictions (note that the material constants determined using previous experiments were not changed).

equivalent stress and strain at the given shear strain rates and compared with the experimental observations. In these predictions from the model, the constants were not changed from the ones determined during the room temperature compression experiments. The model predictions are close to the observed response. The use of von-Mises equivalent stress is an assumption which needs to be investigated later.

5. Conclusions

The compressive uniaxial behavior of the polymer Adiprene-L100 was modeled for quasi-static and dynamic operating conditions, as well as, the stress relaxation experiments using a modified form of MSP and a modified standard solid model developed in this study. Modified standard solid model was also used to capture the response of Adiprene-L100 at different temperatures under quasi-static loadings. The correlations obtained for the modified standard solid model were much better than those by the modified MSP especially in the dynamic strain rate regime and/or at finite deformations. For the stress drop during relaxation periods, the two models were found to be quite comparable for lower strain levels, but at large deformations the new model had much better results. Modeling of experimental observations at a specific strain rate for different temperatures was also performed on the polymer by employing springs with temperature dependent constants and dashpots with viscosity term to incorporate temperature effects. The new model correlations were in fairly good agreement with the experimental observations. Predictions, using the model constants determined from the uniaxial compression experiments, were performed on a compressive strain rate jump experiment, on compressive multiple relaxation experiment and also on free end pure torsion experiments. These predictions, in each case, were very close to the experimental observations. Thus, the model was able to predict the response of the polymeric material very well for quasi-static

experiments at room as well as above and below the glass transition temperature regimes, over a wide range of strain rates, and single and multiple stress relaxation experiments.

This modified viscoelastic new model has a foundation on the infinitesimal linear theory (standard solid model) with a semi-empirical modification based on experimental observations. This implies that the various parameters used in the model have a clear physical insight. In synthesis, the new model developed in this work presents a simple and flexible framework to model nonlinear viscoelastic systems under finite deformation over a wide range of strain rates and temperatures. This model can also be a basis for later generalizations to three-dimensional cases.

References

Argon, A.S., Butalov, V.V., Mott, P.H., Suter, U.W., 1995. Plastic deformation in glassy polymers by atomistic and microscopic simulations. J. Rheol. 39, 377–399.

Bardenhagen, S.G., Stout, M.G., Gray, G.T., 1997. Three-dimensional, finite deformation, viscoplastic constitutive models for polymeric materials. Mech. Mater. 25, 235–253.

Bergstrom, J.S., Boyce, M.C., 1998. Constitutive modeling of the large strain time-dependent behavior of elastomers. J. Mech. Phys. Solids 46, 931–954.

Bird, R.B., Armstrong, R.C., Hassager, O., 1977Dynamics of Polymeric Liquids, vol. 1. Wiley, New York.

Boyce, M.C., Parks, D.M., Argon, A.S., 1988. Large inelastic deformation of glassy polymers, Part I: rate dependent constitutive model. Mech. Mater. 7, 15–33.

Caruthers, J.M., Adolf, D.B., Chambers, R.S., Shrikhande, P., 2004. A thermodynamically consistent, nonlinear viscoelastic approach for modeling glassy polymers. Polymer 45, 4577–4597.

Christensen, R.M., 1982. Theory of Viscoelasticty: An Introduction. Academic Press, New York.

Colak, O., 2005. Modeling deformation behavior of polymers with viscoplasticity theory based on overstress. Int. J. Plasticity 21, 145–160.

Drozdov, A.D., Dorfmann, A., 2003. A micro-mechanical model for the response of filled elastomers at finite strains. Int. J. Plasticity 19, 1037–1067.

Ehlers, W., Markert, B., 2003. A macroscopic finite strain model for cellular polymers. Int. J. Plasticity 19, 961–976.

Findley, W.N., 1968. Product form of kernel functions for nonlinear viscoelasticity of PVC under constant rate stressing. Trans. Soc. Rheol. 12 (2), 217–242.

Flügge, W., 1967. Viscoelasticity. Blaisdel Publishing Company.

Gray III, G.T., Blumenthal, W.R., Trujillo, C.P., Carpenter, R.W., 1997. Influence of temperature and strain rate on the mechanical behavior of Adiprene-L100. Report No. LA-UR-97-0905. Las Alamos National Laboratory.

Green, A.E., Rivlin, R.S., 1957. The mechanics of non-linear materials with memory; Part I. Arch. Ration. Mech. Anal. 1, 1.

Haupt, P., Lion, A., Backhaus, E., 2000. On the dynamic behavior of polymers under finite strains: constitutive modeling and identification of parameters. Int. J. Solids Struct. 37, 3633–3646.

Khan, A.S., Suh, Y.S., Kazmi, R., 2004. Quasi-static and dynamic loading responses and constitutive modeling of titanium alloys. Int. J. Plasticity 20, 2233–2248.

Khan, A.S., Zhang, H., 2001. Finite deformation of a polymer and constitutive modeling. Int. J. Plasticity 17, 1167–1188.

Krempl, E., Khan, F., 2003. Rate (time)-dependent deformation behavior: an overview of some properties of metals and solid polymers. Int. J. Plasticity 19, 1069–1095.

Lai, J.S.Y., Findley, W.N., 1968. Stress relaxation of nonlinear viscoelastic material under uniaxial strain. Trans. Soc. Rheol. 12, 259–280.

Liang, R., Khan, A.S., 1999. A critical review of experimental results and constitutive models for BCC and FCC metals over a wide range of strain rates and temperatures. Int. J. Plasticity 15 (9), 963–980.

Lion, A., 2001. Thermomechanically consistent formulations of the standard linear solid using fractional derivatives. Arch. Mech., 53.

Lion, A., Kardelky, C., 2004. The Payne effect in finite viscoelasticity: constitutive modeling based on fractional derivatives and intrinsic time scales. Int. J. Plasticity 20, 1313–1345.

Liu, Y., Gall, K., Dunn, M.L., Greenberg, A.R., Diani, J., 2006. Thermomechanics of shape memory polymers: uniaxial experiments and constitutive modeling. Int. J. Plasticity 22 (2), 279–313.

Lockett, F.J., 1972. Nonlinear Viscoelastic Solids. Academic Press, London.

Lopez-Pamies, O., Khan, A.S., 2002. Time and temperature dependent response and relaxation of a soft polymer. Int. J. Plasticity 18, 1359–1372.

Lubarda, V.A., Benson, D.J., Meyers, M.A., 2003. Strain-rate effects in rheological models of inelastic response. Int. J. Plasticity 19, 1097–1118.

Makradi, A., Ahzi, S., Gregory, R.V., Edie, D.D., 2005. A two-phase self-consistent model for the deformation and phase transformation behavior of polymers above the glass transition temperature: application to PET. Int. J. Plasticity 21, 741–758.

McGuirt, C., Lianis, G., 1970. Constitutive equations for viscoelastic solids under finite uniaxial and biaxial deformations. Trans. Soc. Rheol. 14 (2), 117–134.

Ogden, R.W., 1997. Non-linear Elastic Deformations. Dover Publications Inc., Mineola, New York.

Painter, P.C., Coleman, M.M., 1997. Fundamentals of Polymer Science: An Introductory Text, second ed. Technomic Publishing Co., Inc..

Pipkin, A.C., Rogers, T.G., 1968. A nonlinear integral representation for viscoelastic behavior. J. Mech. Phys. Solids 16, 59–72.

Rault, J., 2000. Origin of the Vogel–Fulcher–Tammann law in glass-forming materials: the α–β bifurcation. J. Non-Cryst. Solids 271, 177–217.

Reese, S., 2003. A micromechanically motivated material model for the thermo-viscoelastic material behavior of rubber-like polymers. Int. J. Plasticity 19, 909–940.

Smart, J., Williams, J.G., 1972. A comparison of single-integral non-linear viscoelasticity theories. J. Mech. Phys. Solids 20, 313–324.

Ward, I.M., Sweeney, J., 2004. An Introduction to the Mechanical Properties of Solid Polymers, second ed. Wiley, New York.